Original Article

The effect of low-magnitude, high-frequency vibration on poly(ethylene glycol)-microencapsulated mesenchymal stem cells

Journal of Tissue Engineering
Volume 9: 1–12

DOI: 10.1177/2041731418800101
journals.sagepub.com/home/tej
SAGE

Sneha Mehta[1], Brooke McClarren[1], Ayesha Aijaz[1], Rabab Chalaby[2], Kimberly Cook-Chennault[3] and Ronke M Olabisi[1]

Abstract

Low-magnitude, high-frequency vibration has stimulated osteogenesis in mesenchymal stem cells when these cells were cultured in certain types of three-dimensional environments. However, results of osteogenesis are conflicting with some reports showing no effect of vibration at all. A large number of vibration studies using three-dimensional scaffolds employ scaffolds derived from natural sources. Since these natural sources potentially have inherent biochemical and microarchitectural cues, we explored the effect of low-magnitude, high-frequency vibration at low, medium, and high accelerations when mesenchymal stem cells were encapsulated in poly(ethylene glycol) diacrylate microspheres. Low and medium accelerations enhanced osteogenesis in mesenchymal stem cells while high accelerations inhibited it. These studies demonstrate that the isolated effect of vibration alone induces osteogenesis.

Keywords

Cell microencapsulation, low-magnitude, high-frequency vibration, osteogenesis, mesenchymal stem cells, differentiation

Date received: 30 June 2018; accepted: 21 August 2018

Introduction

Low-magnitude, high-frequency (LMHF) vibration has shown anabolic effects on bone when applied to the whole body in both animal and human studies. In animals, accelerated fracture healing has been demonstrated and increases in both bone area and bone density have been observed,[1–6] and in humans, significant increases in hip bone mineral density (BMD) and reductions in bone loss in the spine and femur have been reported.[7,8] Such results led to investigations of the efficacy of LMHF vibrations in growing bone and osteoporotic bone. In randomized clinical trials, there were conflicting results with only modest increases in the BMD of children and adolescents, with no overall effect in young adults[9] and no change in the BMD or bone structure in postmenopausal women.[10,11] In animal models of disuse and osteoporosis, the anabolic effects in bone of LMHF vibrations were also attenuated. LMHF vibrations failed to produce a detectable anabolic effect nor did it mitigate bone loss that was induced by a decline in muscle activity in normal mice.[12] When vibration was applied in conjunction with preventive treatments for osteoporosis and osteopenia (alendronate, estrogen, raloxifene), there was decreased bone loss and improved trabecular architecture when compared to drug therapy alone, but there was very reduced effect when vibration was given without the drug treatment.[13,14] These conflicting results illustrate that the efficacy and optimal parameters for applying LMHF vibrations remain uncertain and as such have prompted large-scale long-term studies to establish the optimal frequency, magnitude, and duration of the LMHF vibration applied for anabolic effects in bone.[15]

[1]Department of Biomedical Engineering, Rutgers University, Piscataway, NJ, USA
[2]Department of Materials Science and Engineering, Rutgers University, Piscataway, NJ, USA
[3]Department of Mechanical and Aerospace Engineering, Rutgers University, Piscataway, NJ, USA

Corresponding author:
Ronke M Olabisi, Department of Biomedical Engineering, Rutgers University, 599 Taylor Road, Piscataway, NJ 08854, USA.
Email: ronke.olabisi@rutgers.edu

Various animal models have relevant pathological conditions that can produce an osteoporotic-like state including the ovariectomy rodent model and the botulinum toxin disuse model. Ovariectiomized rodents undergoing whole body vibration (90 Hz, 0.3 g, 10 min/day) displayed increases in osteoblast activity. The rates of osteogenesis were 159% greater in 90 Hz rats when compared to 45 Hz rats and the non-vibrated controls. In addition, the bone morphology of the 90 Hz rats had the highest trabecular bone volume and thickest trabeculae.[2] In another study, 3 weeks of whole body vibration increased trabecular bone in mice undergoing vibration at 0.3 g while mice undergoing 0.6 g whole body vibration did not demonstrate such increases.[16] These results suggest that the anabolic response depends on both frequency and acceleration magnitudes. These differing results are also observed in in vitro analyses of LMHF vibrations, with some studies showing no effect and others showing increased differentiation of progenitor cells toward an osteogenic lineage.[4,5,17–19] However, the stimulation parameters when applying LMHF vibrations to cell culture vary widely, and some of the differing responses may be linked to the differing conditions of the experiments.[17,20,21] For instance, LMHF vibration studies on cell culture have reported differing vibration frequencies, accelerations, culture conditions, for example, in two-dimensional (2D) monolayer on tissue culture polystyrene (TCPS) versus in three-dimensional (3D) entrapped within scaffolds, and scaffold conditions, for example, natural versus synthetic.[17,20,21] As such, there have been conflicting results observed in viability, growth factor expression, response to stimuli, and differentiation when mesenchymal stem cells (MSCs) subjected to LMHF vibrations are cultured in 3D systems versus 2D systems.[17,20,21] It is understood that cells behave differently in their native environments or when cultured in scaffolds than when cultured on TCPS.[22–26] Similarly, when cells are subjected to vibration in situ, they respond differently to the same vibration when it is delivered in vitro with substrate type and acceleration magnitude affecting outcome.[18,19,22,27,28] Furthermore, vibrated cells on TCPS do not necessarily behave the same between similar investigations. In several LMHF studies, osteogenesis was increased significantly when MSCs on TCPS were vibrated at accelerations of 0.3 g at 35 or 45 Hz.[4,5] Conversely, in other studies that vibrated MSCs on TCPS with 0.3 g accelerations at 30 or 60 Hz, osteogenesis was inhibited.[18,19] In examinations comparing ranges of vibration frequencies and accelerations, proliferation rates increased as frequency increased for 0.2 and 0.3 g, but not for other accelerations.[19,28] Furthermore, the examinations revealed different MSC behavior when seeded in the 3D collagen scaffolds compared to TCPS. In particular, although Collagen I, osteoprotegerin, and vascular endothelial growth factor expression were significantly increased in vibrated groups compared to non-vibrated controls, this was only observed in MSCs cultured on collagen scaffolds. These differing results suggest vibration parameters as well as additional factors, such as microarchitectural differences between scaffolds and TCPS, may influence the mechanotransduction of vibration. Scaffolds may provide a more accurate and consistent in situ representation of the MSC response to vibration.

Cells cultured on TCPS have no microarchitectural or biological cues provided to them on the substrate, thus it can be concluded that any observed response to LMHF vibrations is only due to the vibration. This is not true for cells vibrated in 3D; the majority of scaffolds used in LMHF vibration studies are hydrogels derived natural polymers such as collagen or decellularized native extracellular matrix (ECM).[19,29,30] These scaffolds often retain the microarchitecture, biocompatibility, and bioactivity of the natural sources from which they are derived.[31] They promote many cellular functions due to their complex microarchitecture and the presence of multiple endogenous factors[32] and multiple studies have demonstrated that biochemical and microarchitectural cues play a major role in regulating bone functionality.[33] These findings suggest that scaffolds from natural sources may themselves promote differentiation due to biochemical and microarchitectural cues.

When applied in vivo, vibrations of 90–100 Hz have been implicated in inducing osteogenesis.[2,15,34] However, when applied in vitro, the effect of these vibrations on MSCs has differed depending on substrate.[35,36] In order to isolate the effect of the scaffold from the effect of the LMHF vibrations on entrapped MSCs and determine whether 100 Hz vibration alone can induce osteogenesis, we used a 3D model lacking an ECM-like microarchitecture or biochemical cues. Furthermore, throughout the study, basal and not differentiation media was used. Here, we examine the effect of three different ranges of LMHF accelerations at 100 Hz when applied to human mesenchymal stem cells (hMSCs) microencapsulated within polyethylene glycol diacrylate (PEGDA), a synthetic polymer having no inherent architectural or biochemical cues that can serve as a "blank slate" to the entrapped cells. The microencapsulated hMSCs were then tested for adipocyte, chondrocyte, and osteoblast differentiation following exposure to LMHF vibrations (Figure 1).

Materials and methods

All reagents were from Sigma-Aldrich unless otherwise noted.

Cell culture

Human telomerase reverse transcriptase immortalized human mesenchymal cells (hTERT-hMSCs) confirmed to be capable of differentiating into adipocytes, chondrocytes,

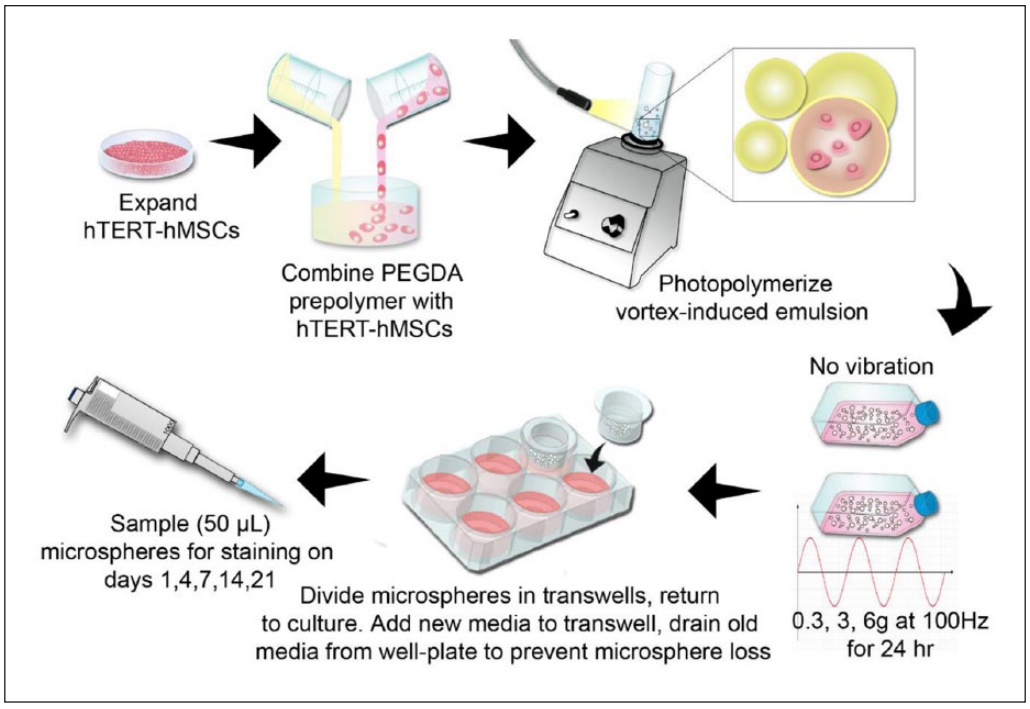

Figure 1. Experimental flow graph. hTERT-MSCs were expanded, harvested, pooled, and then combined with an aqueous PEGDA prepolymer solution containing photoinitiators. This solution was combined with a hydrophobic solution containing photoinitiators, vortexed under white light to polymerize cell-laden microdroplets within the emulsion. Resulting cell-laden microspheres were placed in 25 cm^2 tissue culture flasks and subjected to vibration or no vibration at room temperature for 24 h. Following vibration, microencapsulated cells were returned to incubators and sampled for evaluation at days 1, 4, 7, 14, and 21. At all times, cells were cultured in basal growth media and never supplemented with inducers of differentiation. All experiments were performed with cells from the same pool, which were then divided after microencapsulation.

and osteoblasts were obtained as a gift from the Glackin Lab (City of Hope, Duarte, CA).[37,38] These cells were isolated from 15-week human fetal bone tissue and bone marrow was purified based on the expression of STRO-1^{bright}/$CD106^+$ or STRO-1^{bright}/$CD146^+$ expression, and the purified cell population was then immortalized with hTERT in a pBABE retroviral insertion vector and stable clones were selected with puromycin.[38] Resulting hTERT-hMSCs maintained the multipotency of fetal MSCs well into high passages. For this study, passages 18–35 were used. hTERT-hMSCs were cultured in complete culture basal medium, α-Minimum Essential Medium (α-MEM containing nucleosides, phenol red, and L-glutamine), supplemented with 15% fetal bovine serum (FBS) and 1% penicillin-streptomycin and were maintained at 37°C and at 5% CO_2 in a humidified incubator.

Cell microencapsulation

Cells were microencapsulated as previously described.[39] Briefly, hMSCs were harvested and combined at 10^4 cells/µL with a hydrogel precursor solution containing 0.1 g/mL 10 kDa PEGDA (10% w/v; Laysan Bio), 37 mM 1-vinyl-2-pyrrolidinone with hydrophilic photoinitiators (1.5% (v/v) triethanolamine and 0.1 mM eosin Y) in HEPES-buffered saline (pH 7.4). A hydrophobic photoinitiator solution (2,2-dimethoxy-2-phenyl acetophenone in 1-vinyl-2-pyrrolidinone; 300 mg/mL) was combined in mineral oil (3 µL/mL, sterile filtered) and then subjected to vortex (2 s) under white light (Edmund Optics MH-100 metal halide lamp, 20 s) to photopolymerize the resulting emulsion. Photopolymerized microspheres were isolated by two washes in complete culture medium followed by 5 min centrifugation at 300*g* and maintained in 25 cm^2 flasks with complete culture medium in a humidified incubator at 37°C with 5% CO_2.

LMHF vibration

LMHF vibrations were achieved using a BOSE ElectroForce 3100 mechanical testing machine. Tissue culture flasks (25 cm^2) containing microspheres were removed from culture and attached to the moving actuator of the device using an in-house built aluminum clamp. Using WinTest software, the actuator delivered 0.3, 3, and 6 g with peak-to-peak displacement amplitudes of 0.0149, 0.149, and 0.298 mm, respectively, at 100 Hz for 24 h at room temperature. Parameters were determined using the equation

$$v = \frac{\pi fD}{2}, a = \frac{D(2\pi f)^2}{9.8}$$

where v is velocity, a is acceleration (g), f is frequency (Hz), and D is zero-to-peak displacement.[40]

To determine the vibration imparted to the free-floating microspheres, a 25 cm^2 tissue culture flask with 5 mL culture media containing microspheres was vibrated at 0.3, 3, and 6 g loads at 100 Hz to observe the fluid dynamics of a system of microencapsulated cells. Microspheres take up to 5–15 min to settle when dispersed in media, thus it was assumed that the displacement of the media was a good approximation of microsphere displacement. The displacement of the media within the flask was measured using a laser interferometer. Several trials at each of the g-loads were obtained and the relative peak-to-peak displacement was recorded. The velocity and acceleration of the displacement curves were determined by taking the first and second derivatives of the displacement curves with the aid of a MATLAB code. Velocity and acceleration were also computed using the above equations for sinusoidal motion.

Control microspheres were not vibrated and kept in the same room on a vibration-isolated bench at room temperature for 24 h. After 24 h, vibrated and the control microspheres were removed from 25 cm^2 tissue culture flasks and placed in Transwells (74 μm membrane size (Corning Netwell inserts) in a 6-well plate with 5 mL of basal medium, and kept in a humidified, 5% CO_2 atmosphere).

Cell viability

The hMSCs in both vibrated and control microspheres were assessed for cell viability on days 1, 4, 7, 14, and 21. Microspheres samples (50 μL) from each time point were incubated in complete culture media with 2 mM calcein acetoxymethyl ester and 4 mM ethidium homodimer-1 (LIVE/DEAD Viability/Cytotoxicity Kit for mammalian cells, Life Technologies) for 10 min at 37°C, 5% CO_2 incubator. Microspheres were then observed under an epifluorescent microscope (Zeiss Axiovert) to see labeled live (green, excitation/emission: 495/515 nm) and dead (red, excitation/emission: 528/617 nm) hMSCs. For each condition, three to six green, red, and phase-contrast channel images were taken, then thresholded and counted using NIH Image J to get percentage viability as 100% × Live Cells ÷ (Live Cells + Dead Cells).

Histochemistry

The hMSCs in both vibrated and control microspheres were assessed for differentiation on days 1, 4, 7, 14, and 21. Microspheres samples (50 μL) from each time point were stained with alkaline phosphatase (ALP), Alizarin red S (ARS), Oil red O, or safranin O. ALP was used as preosteoblastic marker while ARS reports the presence of mature osteoblasts through ARS staining of calcium deposits. Oil red O staining was used to identify mature adipocytes by staining lipid droplets, while safranin O staining is used to identify chondrocytes by staining glycosaminoglycans (GAGs). To prevent microsphere loss, vibrated and control microsphere samples were stained in 12-well Transwells (74 μm membrane size Corning Netwell inserts). Reagents and washes were added to the Transwell inserts and aspirated from containing well plates without disturbing the microspheres.

ALP staining. Cells were stained for ALP on day 4 following vibration using a Fluorescence Alkaline Phosphatase Detection Kit. Briefly, microspheres were washed with phosphate-buffered saline (PBS; pH 7.4, containing TWEEN®) (PBST) followed by fixation of cells using their fixation buffer for 5 min, another PBST wash, and finally incubating the microspheres with the staining solution for 30 min. Stained microspheres were imaged using bright-field color microscopy (three to six images per condition). ALP-positive cells stain purple and the stained cells were observed in PBS in a 12-well plate under bright-field microscopy. Images of ALP-positive cells were obtained and all positive cells were counted using NIH Image J counter.

Alizarin red staining. Microsphere samples were washed with PBS, fixed with 10% neutral buffered formalin solution for 15 min, and then washed with distilled water. Then, microsphere samples were stained with 2% (w/v) ARS solution (certified by biological stain commission, Sigma) for 30 min, followed by two distilled water washes. Positively stained calcium deposits appear red in color and were imaged in distilled water in a 12-well plate under bright-field color microscopy (three to six images per condition). Images were analyzed with NIH Image J software. Stain was quantified by counting microspheres containing positive Alizarin red and total microspheres per field then dividing number of microspheres containing positive stain by total microspheres counted. Percentages were averaged and reported as mean ± standard error.

Oil red O staining. Microsphere samples were washed with PBS, fixed with 10% neutral buffered formalin solution for 15 min, washed with distilled water, and then washed with 0.6% (v/v) isopropanol. Microsphere samples were then incubated with 0.3% (v/v) Oil red O solution (certified by biological stain commission, Sigma) for 15 min, followed by two to three washes with distilled water. Positively stained lipid droplets appear red in color. Stained microspheres were imaged in distilled water in a 12-well plate under bright-field color microscopy (three to six images per condition). Images were analyzed with NIH Image J software. Images of Oil red O-positive

Table 1. Displacement, velocity, and acceleration of media with microspheres.

Displacement (mm)		Velocity (mm/s)			Acceleration (g)		
Applied	Actual	Applied	Sinusoidal	RMS	Applied	Sinusoidal	RMS
0.0149	0.004 ± 0.0005	4.68	1.38 ± 0.16	0.27 ± 0.03	0.3	0.09 ± 0.01	0.005 ± 0.004
0.149	0.002 ± 0.0002	46.81	0.69 ± 0.06	0.19 ± 0.01	3	0.04 ± 0.004	0.006 ± 0.00009
0.298	0.001 ± 0.0002	93.62	0.31 ± 0.06	0.21 ± 0.02	6	0.02 ± 0.004	0.01 ± 0.00009

RMS: root mean square.

microspheres were obtained and all positive microspheres were counted using NIH Image J counter.

Safranin O staining. Microsphere samples were washed with PBS, fixed with 10% neutral buffered formalin solution for 15 min, and then washed with distilled water. Microsphere samples were then incubated with 0.6% (v/v) safranin O for 10–12 min and then washed twice with distilled water. Safranin O stains sulfated GAGs in chondrocytes an orange color. Stained microspheres were observed in distilled water in a 12-well plate under bright-field color microscopy (three to six images per condition). Images were analyzed with NIH Image J software.

Statistical analysis

For cell viability and Alizarin red analysis, all data were obtained in triplicate and reported as mean ± standard error. For ALP activity, all positive cells in a sample were imaged and counted. A Student's t-test was performed when comparing two groups or an analysis of variance (ANOVA) when comparing more than two groups. Following ANOVA, pairwise comparisons between groups was performed using Tukey's post hoc analysis. p-values less than 0.05 were considered significant and are indicated in the figures with asterisks. Analyses were conducted using Microsoft Excel.

Results

Cell culture model

Microsphere size and density of entrapped cells was assessed via NIH ImageJ to better describe the 3D environment of the microencapsulated cells. Microspheres produced were polydisperse, with most ranging in diameter from 50 to 300 μm, as has been previously reported.[39] Cell density per microsphere was also non-uniform with <5% of microspheres having 0–10 cells in them. The majority of microspheres contained cells that comprised 46%–76% ± 5.3%–4.2% of the total microsphere volume. Less than 5% contained cells comprising 80%–90% of the microsphere volume. Microspheres with very few cells displayed low cell viability and hMSCs entrapped within microspheres did not proliferate.

LMHF vibration

The displacement of the media containing microspheres was measured with a laser interferometer to better describe the motion imparted to the cells. Between 7 and 9 trials of data were captured for 0.3, 3, and 6 g vibration at 100 Hz and averaged. The highest and lowest values of peak-to-peak displacement were excluded from the averaged values. The peak-to-peak displacement for each of the trials, root mean square (RMS) of the velocity, and RMS of the acceleration are provided in Table 1. Representative graphs of vertical displacement, velocity, and acceleration of the media containing microspheres are provided in Figure 2.

In addition to calculating the first and second derivatives of motion, the equations for sinusoidal motion were used to determine the velocity and acceleration of the media from measured values. These values in addition to the peak-to-peak displacement for each of the trials, RMS of the velocity, and RMS of the acceleration are provided in Table 1. The media only achieved 29.5% ± 1.5%, 1.5% ± 0.6%, and 0.34% ± 0.03% of the imparted displacement for 0.3, 3, and 6 g, respectively. The sinusoidal acceleration of the media was inversely proportional to the acceleration of the tissue culture flask, decreasing with applied g, while the RMS acceleration was directly proportional to the flask acceleration.

Cell viability

The viability of LMHF-vibrated and control (0 g) microencapsulated hTERT-MSC samples ranged from 70%–80% ± 1.7%–2.4% on day 1 and reduced to 48%–54% ± 2.6%–3.3% on day 21 (Figure 3). A maximum viability of 80% ± 2.4% was seen at day 1 in the 0.3 g group and a minimum viability of 48% ± 2.6% was observed in 6 g samples on day 21. All groups decreased in viability over time. There was no statistical difference between groups on any days. The live cells were stained green by fluorescent calcein-AM dye and dead cells were stained red by fluorescent ethidium homodimer-1 dye (Figure 2).

Histochemistry

ALP and Alizarin red staining was performed to evaluate the progress of osteogenesis differentiation (Figures 4

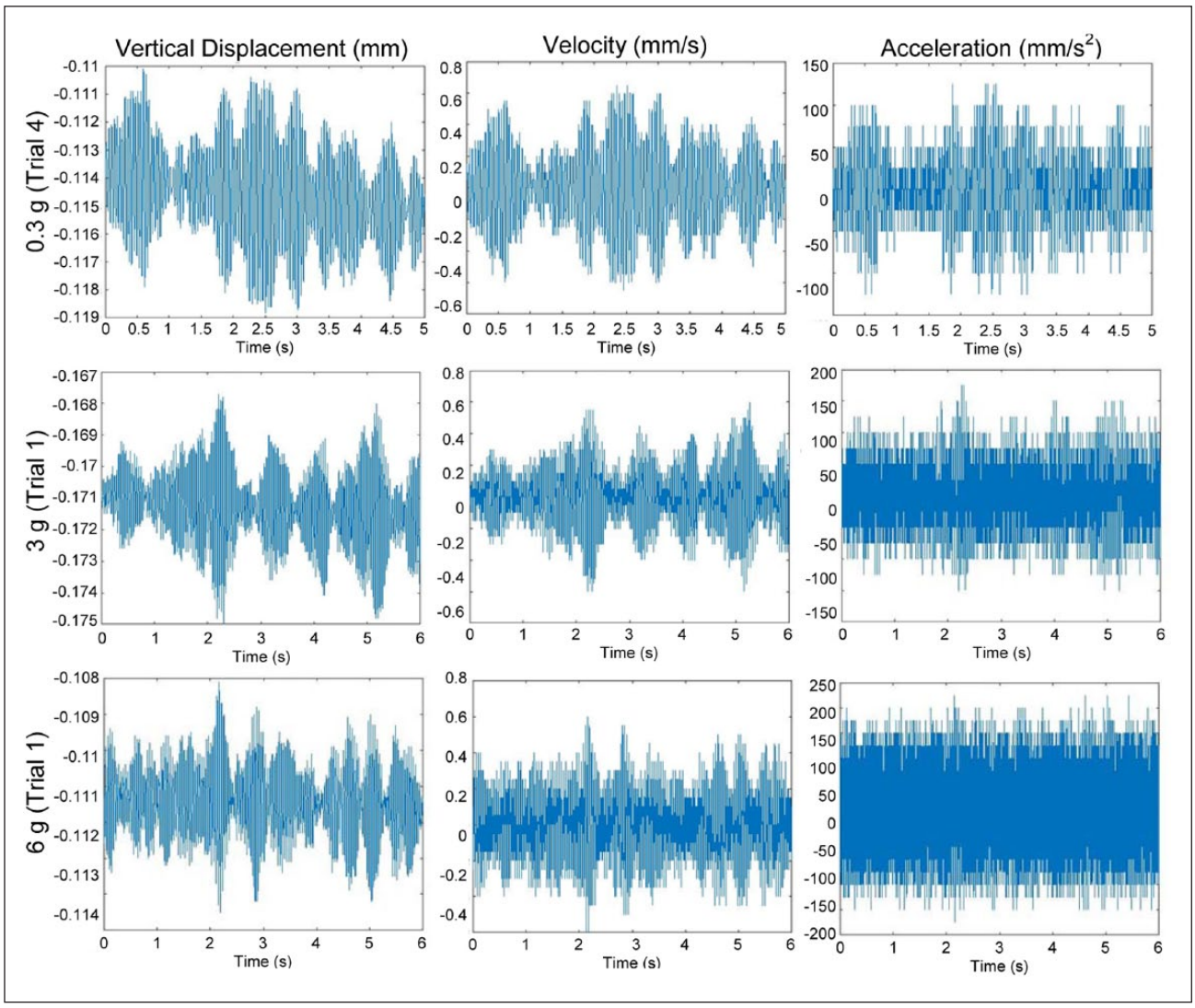

Figure 2. Representative graphs of vertical displacement (left column), velocity (middle column), and acceleration (right column) for 0.3 g (top row), 3 g (middle row), and 6 g (bottom row) of the media containing microspheres.

and 5). LMHF-vibrated hTERT-hMSCs did not show any evidence of differentiation into chondrocytes or adipocytes and all stained microspheres were negative for both Oil red O stain (Figure 6) and safranin O stain (Figure 7). Control non-vibrated cells did, however, show positive Oil red O stain and both non-vibrated and vibrated cells displayed evidence of osteogenic differentiation. After the application of LMHF vibrations, ALP staining observed in hTERT-hMSC increased significantly in vibrated groups over control for 0.3 and 3 g groups, while ALP expression decreased significantly compared to control in the 6 g group (Figure 4). ALP activity was greatest for 0.3 g and decreased with increasing vibration magnitude. Because ALP activity was modest, all cells that were positive were imaged and counted.

There was no ARS staining detected in either vibrated or control groups in the first 7 days following exposure to LMHF vibration. On days 14 and 21, however, ARS-positive microspheres were observed in both vibrated and control groups (Figure 5). Positive stain is reported as number of microspheres containing positive stain ÷ total microspheres counted. ARS-positive microspheres increased in all groups from day 14 to day 21, but significantly higher staining was observed in vibrated groups when compared to control. The 6 g group did not stain positive on day 14. ARS-positive microspheres were highest in the 0.3 g vibration group on days 14 and 21. Positive staining decreased with an increase in the intensity of vibration.

Oil red O stain did not appear in any microspheres until day 21 and was only present in a total of seven (an average of 2.3 ± 0.7) control non-vibrated microspheres (Figure 6). Because Oil red O stain was low, all microspheres that were positive were imaged and counted.

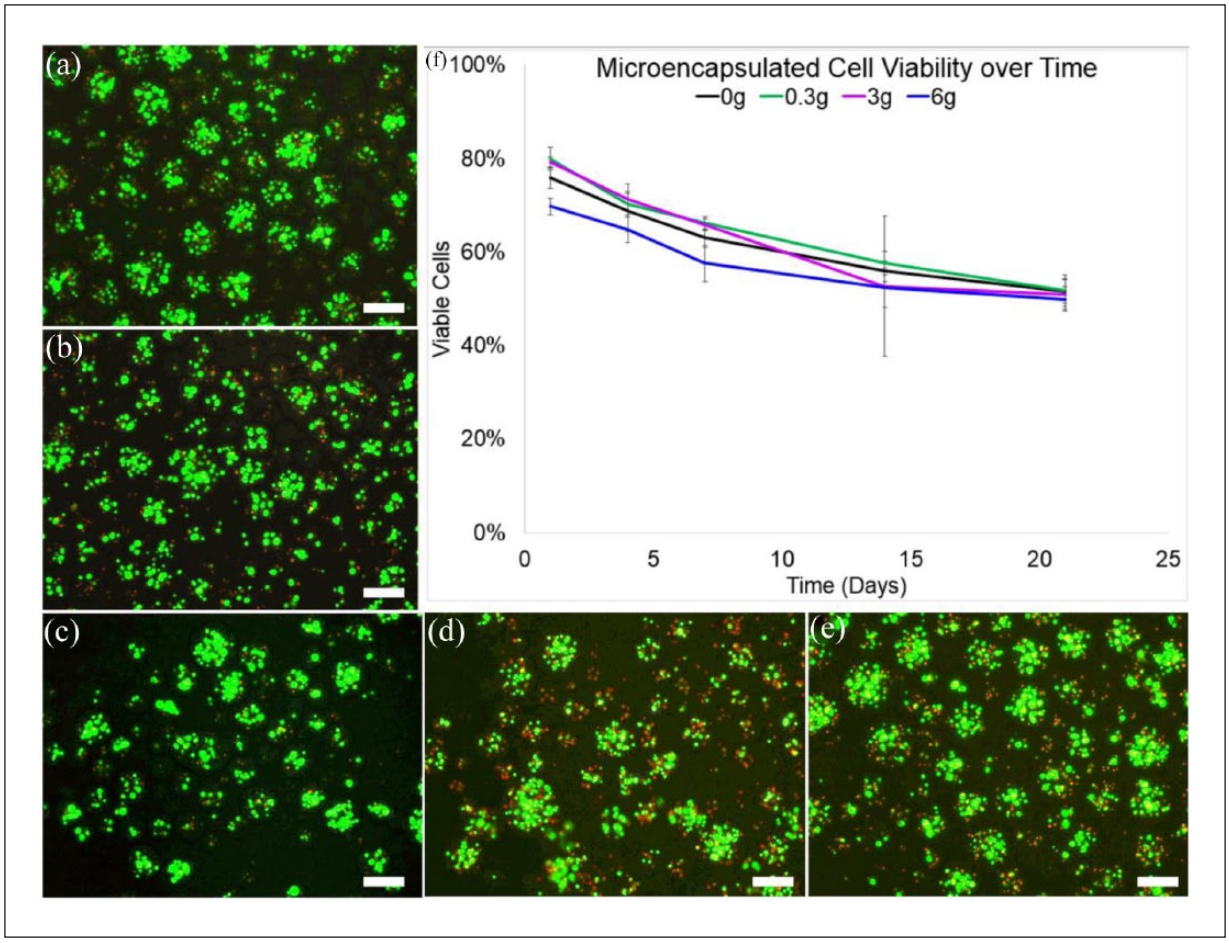

Figure 3. Cell viability of LMHF 0.3 g vibrated microencapsulated hTERT-hMSCs on days (a) 1, (b) 4, (c) 7, (d) 14, and (e) 21 following vibration (f) Percent cell viability of all treatment groups, 0 (control), 0.3, 3, and 6 g plotted against time. Green indicates live cells, and red indicates dead cells. The maximum viability (80% ± 2.4%) was observed in 0.3 g microsphere samples on day 1 and minimum viability (48% ± 2.4%) was observed in 6 g microsphere samples on day 21. There was no statistical difference between groups. Viability declined over time. Images were adjusted for contrast and brightness. Scale bars are 100 µm. Error bars indicate standard error.

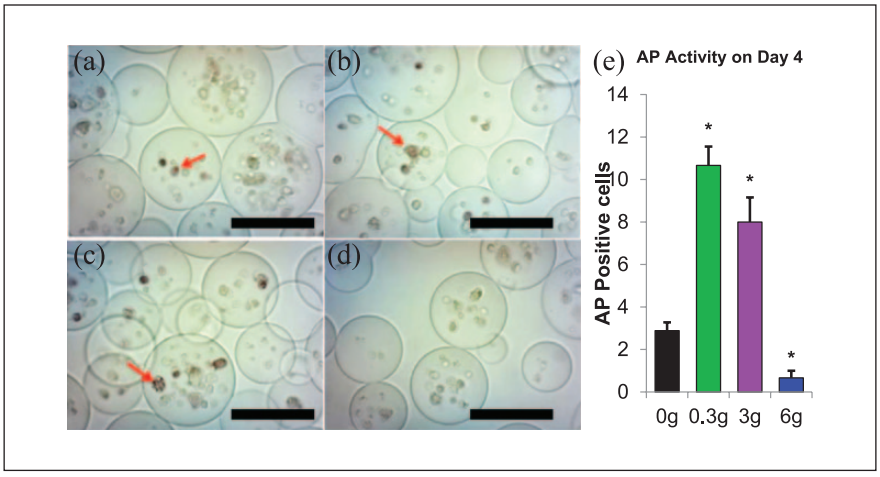

Figure 4. Alkaline phosphatase staining on day 4 for (a). Control (0 g) and vibrated groups ((b) 0.3 g, (c) 3 g, and (d) 6 g). Red arrows indicate ALP-positive purple-colored cells. (e) All ALP-positive cells within each 50 µL microsphere sample were counted from images. Scale bars are 100 µm. Error bars show standard error of mean. Asterisks show significant difference from control.

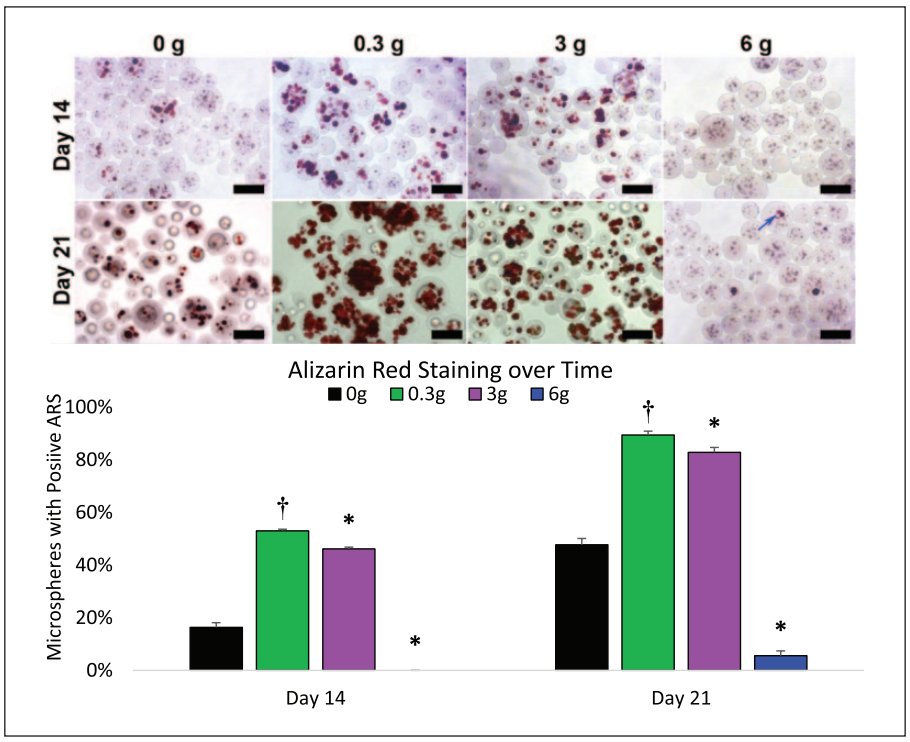

Figure 5. Alizarin Red S staining for vibrated and control (0 g) groups on days 14 and 21. Red stain of positively stained calcium deposits is present throughout 0–3 g acceleration; the arrow indicates red color in the 6 g group. The onset of mineralization was accelerated in 0.3 and 3.0 g vibrated groups compared to non-vibrated controls. Microspheres were counted from images (3–6 images per group). Graph shows percent microspheres showing positive ARS stain (positive microspheres ÷ total microspheres). There was no positive staining detected in 6 g vibrated groups on day 14 and very little detected on day 21. Images were adjusted for brightness and contrast. Crosses indicate statistically significant difference ($p < 0.05$) compared to all other groups. Asterisks indicate statistically significant difference compared to control. Scale bars are 100 µm. Error bars show standard error of mean.

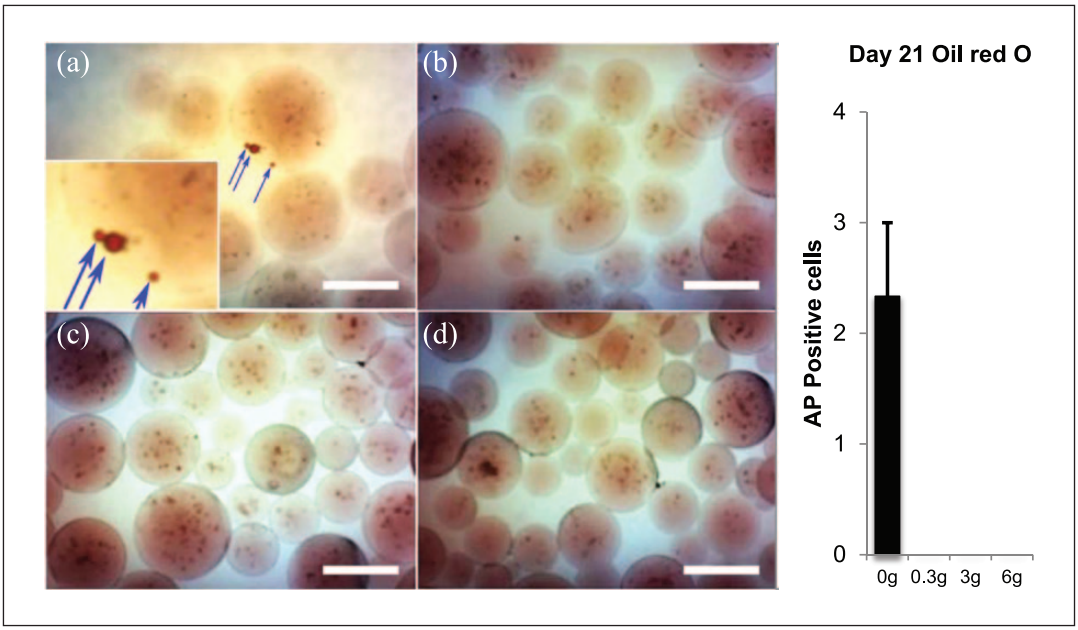

Figure 6. Oil red O staining for day 21 for (a). Control (0 g) and vibrated groups ((b) 0.3 g, (c) 3 g, and (d) 6 g). Blue arrows indicate Oil red O-positive red-colored lipid droplets. Due to the 3D nature of the microspheres, the lipid droplets appear as spherical stains distinct and separate from cells (inset). There were only a total of seven microspheres (an average of 2.3 ± 0.7) with positive Oil red O stain counted in all the samples, with all seven from the control non-vibrated group. These droplets did not appear until day 21. Images were adjusted for brightness and contrast. Scale bars are 100 µm.

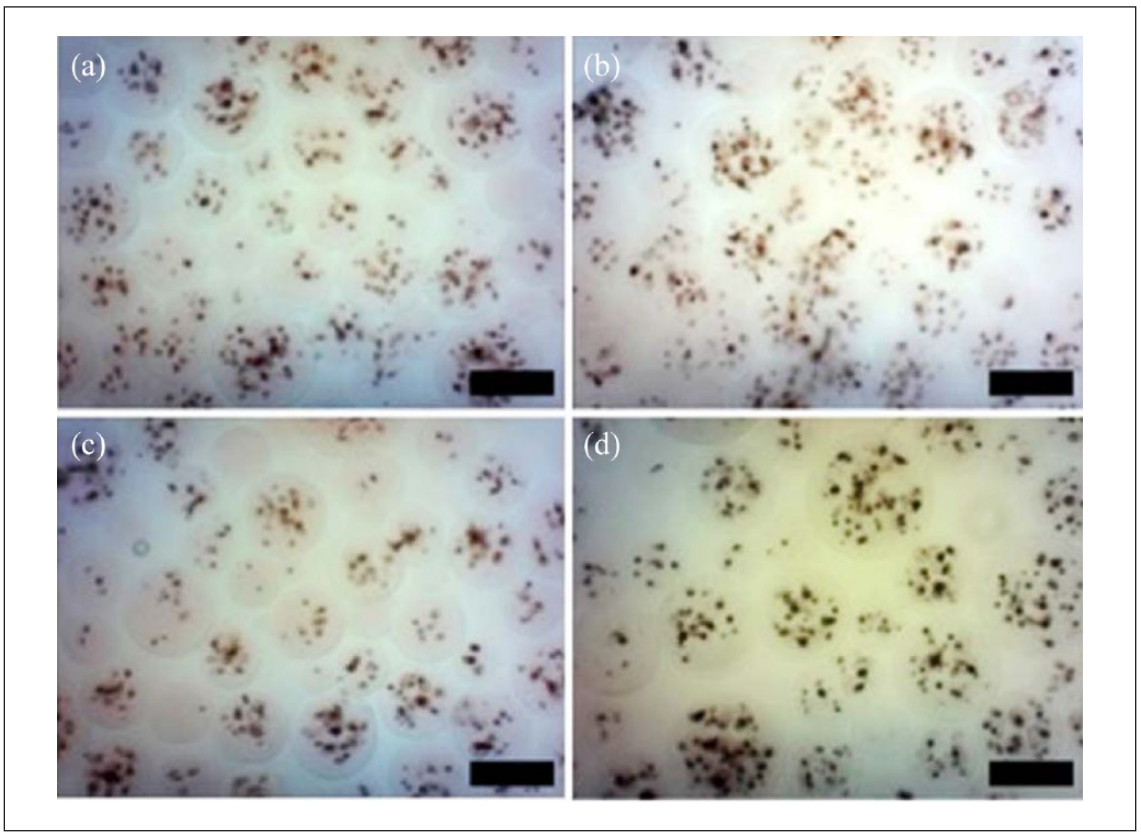

Figure 7. Safranin O staining for day 21 for (a). Control (0 g) and vibrated groups ((b) 0.3 g, (c) 3 g, and (d) 6 g). The sulfated glycosaminoglycans characteristic of differentiated chondrocytes, if stained, appear orange. There was no positive staining detected at any time point for any group. Images were adjusted for brightness and contrast. Scale bars are 100 µm.

Discussion

This study investigated the effect of a range of accelerations delivered via LMHF vibration on PEGDA-encapsulated hTERT-hMSCs. hTERT-hMSCs were selected over primary adult MSCs because fetal MSCs express pluripotency markers, grow faster, and when immortalized, can be passaged to very high passages with little changes in cell behavior.[41] We previously demonstrated that when these microencapsulated hTERT-hMSCs were cultured in osteogenic media containing calcein (1 µg/mL), the fluorescence of calcein incorporated into the extracellular mineral ingredients could be visualized with an epifluorescent microscope and that this fluorescence was colocalized with Alizarin red stain.[42] Since calcein staining for mineralization precludes the use of calcein AM staining for viability, here we only used Alizarin red stain for mineralization. In addition, in preliminary studies comparing viability assessments, we found no statistical difference in viability measurements when using confocal versus epifluorescent microscopy for identical samples, hence we used epifluorescent microscopy throughout. The viability of both control and vibrated microspheres declined over time, as expected, since cells do not proliferate in these hydrogels.[43]

Multiple biochemical and biophysical cues have been employed to direct the differentiation of MSCs. Biochemical signals and their concomitant cell responses are well known and commonly employed by investigators to successfully specify cell differentiation. In particular, it is well known that osteogenesis in MSCs is promoted by inclusion of dexamethasone, ascorbic acid and beta-glycerophosphate, or bone morphogenetic proteins in the media. Biophysical cues to guide MSC differentiation are still being described. It is well known that scaffold stiffness comparable to native tissues can be used to guide specific-lineage differentiation of MSCs as effectively as chemical factors. For instance, MSCs underwent osteogenesis, myogenesis, and neurogenesis when cultured on substrates with elastic moduli resembling bone, muscle, and neural tissues, respectively.[44] Conversely, when undergoing cyclic loading such as vibration or cyclic tensile strain, results are broadly conflicting. MSCs subjected to similar tensile strain undergo myogenesis, tenogenesis, and osteogenesis, while the fate of MSCs subjected to vibration depended largely upon the substrate.[17]

Amid varying reports of whether LMHF vibration induces osteogenesis in MSCs in 3D culture, our motivation was to examine the response of these cells in a synthetic

polymer devoid of microarchitecture or signaling molecules to isolate the response of these cells to vibration. Such use of PEGDA as a "blank slate" due to the polymer's lack of cell adhesion sites and non ECM-like structure[45,46] ensures that during the vibration period, encapsulated cells receive no microarchitectural or biochemical cues capable of stimulating MSC differentiation, as has been reported for MSCs encapsulated in natural polymers.[24] Moreover, the PEGDA-microencapsulated hTERT-hMSCs were maintained in MSC proliferation media and were not exposed to osteogenic media, which contains the chemical stimulators dexamethasone, ascorbic acid, and beta-glycerophosphate. Without any media or scaffold inducers of differentiation, our study was poised to determine whether LMHF vibration alone is a sufficient stimulus to drive the differentiation of MSCs.

Of the conditions tested, LMHF vibrations with low acceleration (0.3 g) enhanced the osteogenic differentiation of encapsulated hTERT-hMSCs more strongly than any other group, as evidenced by increased ALP activity, accelerated onset of mineralization, and increased levels of mineralization. Vibrated cells failed to differentiate into chondrocytes or adipocytes, though they were confirmed capable of such differentiation when incubated in differentiation media. Thus, we can conclude that the applied LMHF vibration was not an inducer of chondrogenesis or adipogenesis. The osteogenesis we observed may have implications for reports where no osteogenesis was observed for MSCs subjected to LMHF vibrations in 3D culture. For instance, it is possible that 100 Hz is ideal for osteogenic differentiation, and LMHF vibration studies range from 10 to 150 Hz.[21] The ranges selected in this study, 0.3 g, 3 g, and 6 g at 100 Hz, were chosen because they were close to the values used in various animal and human whole body vibration studies.[2,5,16,47–51] The 100 Hz frequency was selected because various animal models have reported osteogenesis at accelerations within the 90–100 Hz frequency range.[2,15,34]

The preferential osteogenic differentiation of control non-vibrated microspheres suggests that the state of being microencapsulated within PEGDA hydrogel microspheres is osteoinductive. Entrapped cells were forced into a rounded morphology, which has been reported to promote adipogenesis rather than osteogenesis.[52,53] Although this may explain evidence of adipogenesis as indicated by the presence of positive Oil red O stained lipid droplets (produced by adipocytes) observed in non-vibrated controls, the differentiation of these cells was overwhelmingly osteogenic. In addition, the entrapped cells are under compression, which induces chondrogenesis instead of osteogenesis;[54] droplets have higher internal pressures due to surface tension, and this pressure combined with the swelling of the material likely exerts compressive forces on the entrapped cells. The most likely cause of the preferential osteogenic differentiation of these hydrogel-entrapped MSCs is due to the elastic modulus of the containing PEGDA microspheres. These hydrogels have an elastic modulus of 100 ± 8 kPa,[55] which is precisely the elastic modulus of precalcified bone.[56] Tension is reported to induce osteogenesis, but most studies reporting tension-induced osteogenesis examine cyclic tension.[17] Although unlikely, it is possible that there is an interfacial tension between the cells and the PEGDA that is enough to induce osteogenesis. Further work is needed to fully describe the loading environment within the microspheres.

The inhibition of mineralization observed in 6 g groups contradicts several animal studies, which reported that higher acceleration (approximately 5 g and above) decreases bone resorption, but has no effect on bone formation.[57] However, this study delivered 24 h of 6 g vibrations, while the animal studies did not, which may account for the difference. The measured acceleration of the media within the flasks was far below 6 g at 0.02 g, and the inhibitory effect of the acceleration suggests that the microspheres were subjected to greater acceleration than that of the media. Future work to mathematically model the movement of the microspheres will better describe the movement of the microspheres at each acceleration to elucidate the effect of acceleration magnitude on MSC differentiation. This work confirmed that low-acceleration LMHF vibration alone can induce osteogenesis without other inducers of osteogenesis. Thus, this study establishes a new 3D culture model for investigating the isolated effects of LMHF vibrations on cells.

Acknowledgements

hTERT-hMSCs were provided as a gift from Carlotta Glackin, City of Hope, Duarte, CA.

Declaration of conflicting interests

The author(s) declared no potential conflicts of interest with respect to the research, authorship, and/or publication of this article.

Funding

The author(s) received no financial support for the research, authorship, and/or publication of this article.

ORCID iD

Ronke M Olabisi https://orcid.org/0000-0003-3738-5250

References

1. Xie L, Jacobson JM, Choi ES, et al. Low-level mechanical vibrations can influence bone resorption and bone formation in the growing skeleton. *Bone* 2006; 39: 1059–1066.
2. Judex S, Lei X, Han D, et al. Low-magnitude mechanical signals that stimulate bone formation in the ovariectomized rat are dependent on the applied frequency but not on the strain magnitude. *J Biomech* 2007; 40: 1333–1339.

3. Xie L, Rubin C and Judex S. Enhancement of the adolescent murine musculoskeletal system using low-level mechanical vibrations. *J Appl Physiol* 2008; 104: 1056–1062.
4. Vanleene M and Shefelbine SJ. Therapeutic impact of low amplitude high frequency whole body vibrations on the osteogenesis imperfecta mouse bone. *Bone* 2013; 53: 507–514.
5. Shi H-F, Cheung W-H, Qin L, et al. Low-magnitude high-frequency vibration treatment augments fracture healing in ovariectomy-induced osteoporotic bone. *Bone* 2010; 46: 1299–1305.
6. Leung KS, Shi HF, Cheung WH, et al. Low-magnitude high-frequency vibration accelerates callus formation, mineralization, and fracture healing in rats. *J Orthop Res* 2009; 27: 458–465.
7. Verschueren SM, Roelants M, Delecluse C, et al. Effect of 6-month whole body vibration training on hip density, muscle strength, and postural control in postmenopausal women: a randomized controlled pilot study. *J Bone Miner Res* 2004; 19: 352–359.
8. Rubin C, Recker R, Cullen D, et al. Prevention of postmenopausal bone loss by a low-magnitude, high-frequency mechanical stimuli: a clinical trial assessing compliance, efficacy, and safety. *J Bone Miner Res* 2004; 19: 343–351.
9. Slatkovska L, Alibhai S, Beyene J, et al. Effect of whole-body vibration on BMD: a systematic review and meta-analysis. *Osteoporos Int* 2010; 21: 1969–1980.
10. Slatkovska L, Alibhai SM, Beyene J, et al. Effect of 12 months of whole-body vibration therapy on bone density and structure in postmenopausal women: a randomized trial. *Ann Inter Med* 2011; 155: 668–679.
11. Lau RW, Liao L-R, Yu F, et al. The effects of whole body vibration therapy on bone mineral density and leg muscle strength in older adults: a systematic review and meta-analysis. *Clin Rehabil* 2011; 25: 975–988.
12. Manske SL, Good CA, Zernicke RF, et al. High-frequency, low-magnitude vibration does not prevent bone loss resulting from muscle disuse in mice following botulinum toxin injection. *PLoS ONE* 2012; 7: e36486.
13. Chen G-X, Zheng S, Qin S, et al. Effect of low-magnitude whole-body vibration combined with alendronate in ovariectomized rats: a random controlled osteoporosis prevention study. *PLoS ONE* 2014; 9: e96181.
14. Stuermer EK, Komrakova M, Sehmisch S, et al. Whole body vibration during fracture healing intensifies the effects of estradiol and raloxifene in estrogen-deficient rats. *Bone* 2014; 64: 187–194.
15. Mikhael M, Orr R and Singh MAF. The effect of whole body vibration exposure on muscle or bone morphology and function in older adults: a systematic review of the literature. *Maturitas* 2010; 66: 150–157.
16. Chan ME, Adler BJ, Green DE, et al. Bone structure and B-cell populations, crippled by obesity, are partially rescued by brief daily exposure to low-magnitude mechanical signals. *FASEB J* 2012; 26: 4855–4863.
17. McClarren B and Olabisi R. Strain and vibration in mesenchymal stem cells. *Int J Biomater* 2018; 2018: 8686794.
18. Chen YJ, Huang CH, Lee IC, et al. Effects of cyclic mechanical stretching on the mRNA expression of tendon/ligament-related and osteoblast-specific genes in human mesenchymal stem cells. *Connect Tissue Res* 2008; 49: 7–14.
19. Kim IS, Song YM, Lee B, et al. Human mesenchymal stromal cells are mechanosensitive to vibration stimuli. *J Dent Res* 2012; 91: 1135–1140.
20. Delaine-Smith RMR and Gwendolen. Mesenchymal stem cell responses to mechanical stimuli. *Muscles Ligaments Tendons J* 2012; 2: 169–180.
21. Edwards JH and Reilly GC. Vibration stimuli and the differentiation of musculoskeletal progenitor cells: review of results in vitro and in vivo. *World J Stem Cells* 2015; 7: 568–582.
22. Kabiri M, Kul B, Lott WB, et al. 3D mesenchymal stem/stromal cell osteogenesis and autocrine signalling. *Biochem Biophys Res Commun* 2012; 419: 142–147.
23. Cukierman E, Pankov R and Yamada KM. Cell interactions with three-dimensional matrices. *Curr Opin Cell Biol* 2002; 14: 633–639.
24. Pedersen JA and Swartz MA. Mechanobiology in the third dimension. *Ann Biomed Eng* 2005; 33: 1469–1490.
25. Bartholomew A, Sturgeon C, Siatskas M, et al. Mesenchymal stem cells suppress lymphocyte proliferation in vitro and prolong skin graft survival in vivo. *Exp Hematol* 2002; 30: 42–48.
26. Gimble JM, Guilak F, Nuttall ME, et al. In vitro differentiation potential of mesenchymal stem cells. *Transfus Med Hemother* 2008; 35: 228–238.
27. Lau E, Lee WD, Li J, et al. Effect of low-magnitude, high-frequency vibration on osteogenic differentiation of rat mesenchymal stromal cells. *J Orthop Res* 2011; 29: 1075–1080.
28. Hwang SJ, Song YM, Cho TH, et al. The implications of the response of human mesenchymal stromal cells in three-dimensional culture to electrical stimulation for tissue regeneration. *Tissue Eng Part A* 2012; 18: 432–445.
29. Zhou Y, Guan X, Zhu Z, et al. Osteogenic differentiation of bone marrow-derived mesenchymal stromal cells on bone-derived scaffolds: effect of microvibration and role of ERK1/2 activation. *Eur Cell Mater* 2011; 22: 12–25.
30. Mauney J, Sjostorm S, Blumberg J, et al. Mechanical stimulation promotes osteogenic differentiation of human bone marrow stromal cells on 3-D partially demineralized bone scaffolds in vitro. *Calcif Tissue Int* 2004; 74: 458–468.
31. Dawson E, Mapili G, Erickson K, et al. Biomaterials for stem cell differentiation. *Adv Drug Deliv Rev* 2008; 60: 215–228.
32. Cushing MC and Anseth KS. Hydrogel cell cultures. *Science* 2007; 316: 1133–1134.
33. Porter JR, Ruckh TT and Popat KC. Bone tissue engineering: a review in bone biomimetics and drug delivery strategies. *Biotechnol Prog* 2009; 25: 1539–1560.
34. Christiansen BA and Silva MJ. The effect of varying magnitudes of whole-body vibration on several skeletal sites in mice. *Ann Biomed Eng* 2006; 34: 1149–1156.
35. Demiray L and Özçivici E. Bone marrow stem cells adapt to low-magnitude vibrations by altering their cytoskeleton during quiescence and osteogenesis. *Turk J Biol* 2015; 39: 88–97.
36. Sen B, Xie Z, Case N, et al. Mechanical signal influence on mesenchymal stem cell fate is enhanced by incorporation of refractory periods into the loading regimen. *J Biomech* 2011; 44: 593–599.

37. Samineni S, Glackin C and Shively JE. Role of CEACAM1, ECM, and mesenchymal stem cells in an orthotopic model of human breast cancer. *Int J Breast Cancer* 2011; 2011: 381080.
38. Nierste BA, Glackin CA and Kirshner J. Dkk-1 and IL-7 in plasma of patients with multiple myeloma prevent differentiation of mesenchymal stem cells into osteoblasts. *Am J Blood Res* 2014; 4: 73–85.
39. Aijaz A, Perera D and Olabisi RM. Polymeric materials for cell microencapsulation. *Methods Mol Biol* 2017; 1479: 79–93.
40. Rauch F, Sievanen H, Boonen S, et al. Reporting whole-body vibration intervention studies: recommendations of the International Society of Musculoskeletal and Neuronal Interactions. *J Musculoskelet Neuronal Interact* 2010; 10: 193–198.
41. Guillot PV, Gotherstrom C, Chan J, et al. Human first-trimester fetal MSC express pluripotency markers and grow faster and have longer telomeres than adult MSC. *Stem Cells* 2007; 25: 646–654.
42. Olabisi R, Finlay J, Lowe G, et al. Novel approach to microencapsulate mesenchymal stem cells to inhibit immune response and repair skeletal defects in patients with cancer induced bone disease. In: *Proceedings of the 10th annual meeting of the International Society for Stem Cell Research*, Yokohama, Japan, 13–16 June 2012.
43. Aijaz A, Faulknor R, Berthiaume F, et al. Hydrogel microencapsulated insulin-secreting cells increase keratinocyte migration, epidermal thickness, collagen fiber density, and wound closure in a diabetic mouse model of wound healing. *Tissue Eng Part A* 2015; 21: 2723–2732.
44. Her GJ, Wu HC, Chen MH, et al. Control of three-dimensional substrate stiffness to manipulate mesenchymal stem cell fate toward neuronal or glial lineages. *Acta Biomater* 2013; 9: 5170–5180.
45. Singh A and Elisseeff J. Biomaterials for stem cell differentiation. *J Mater Chem* 2010; 20: 8832–8847.
46. Salinas CN, Cole BB, Kasko AM, et al. Chondrogenic differentiation potential of human mesenchymal stem cells photoencapsulated within poly(ethylene glycol)-arginine-glycine-aspartic acid-serine thiol-methacrylate mixed-mode networks. *Tissue Eng* 2007; 13: 1025–1034.
47. Von Stengel S, Kemmler W, Engelke K, et al. Effects of whole body vibration on bone mineral density and falls: results of the randomized controlled ELVIS study with postmenopausal women. *Osteoporos Int* 2011; 22: 317–325.
48. Lau E, Al-Dujaili S, Guenther A, et al. Effect of low-magnitude, high-frequency vibration on osteocytes in the regulation of osteoclasts. *Bone* 2010; 46: 1508–1515.
49. Uzer G, Pongkitwitoon S, Ian C, et al. Gap junctional communication in osteocytes is amplified by low intensity vibrations in vitro. *PLoS ONE* 2014; 9: e90840.
50. Garman R, Gaudette G, Donahue LR, et al. Low-level accelerations applied in the absence of weight bearing can enhance trabecular bone formation. *J Orthop Res* 2007; 25: 732–740.
51. Castillo AB, Alam I, Tanaka SM, et al. Low-amplitude, broad-frequency vibration effects on cortical bone formation in mice. *Bone* 2006; 39: 1087–1096.
52. Mathieu PS and Loboa EG. Cytoskeletal and focal adhesion influences on mesenchymal stem cell shape, mechanical properties, and differentiation down osteogenic, adipogenic, and chondrogenic pathways. *Tissue Eng Part B: Rev* 2012; 18: 436–444.
53. Kilian KA, Bugarija B, Lahn BT, et al. Geometric cues for directing the differentiation of mesenchymal stem cells. *Proc Natl Acad Sci* 2010 Mar 16; 107(11): 4872–4877.
54. Kelly DJ and Jacobs CR. The role of mechanical signals in regulating chondrogenesis and osteogenesis of mesenchymal stem cells. *Birth Defects Res C: Embryo Today* 2010; 90: 75–85.
55. White C, DiStefano T and Olabisi R. The influence of substrate modulus on retinal pigment epithelial cells. *J Biomed Mater Res A* 2017; 105: 1260–1266.
56. Murphy CM, Matsiko A, Haugh MG, et al. Mesenchymal stem cell fate is regulated by the composition and mechanical properties of collagen–glycosaminoglycan scaffolds. *J Mech Behav Biomed* 2012; 11: 53–62.
57. Nowak A, Łochyński D, Pawlak M, et al. High-magnitude whole-body vibration effects on bone resorption in adult rats. *Aviat Space Environ Med* 2014; 85: 518–521.